

# Label-free Detection for a DNA Methylation Assay Using Raman Spectroscopy

Jeongho Kim<sup>1</sup>, Hae Jeong Park<sup>2</sup>, Jae Hyung Kim<sup>1</sup>, Boksoon Chang<sup>3</sup>, Hun-Kuk Park<sup>1,4</sup>

<sup>1</sup>Department of Biomedical Engineering, College of Medicine, Kyung Hee University, Seoul 02447, Korea

<sup>2</sup>Department of Pharmacology, College of Medicine, Kyung Hee University, Seoul 02447, Korea

<sup>3</sup>Department of Pulmonary and Critical Care Medicine, Kyung Hee University Hospital at Gangdong, Seoul 05278, Korea

<sup>4</sup>Department of Medical Engineering, Graduate School, Kyung Hee University, Seoul 02447, Korea

Jeongho Kim and Hae Jeong Park contributed equally to this work.

## Abstract

**Background:** DNA methylation has been suggested as a biomarker for early cancer detection and treatment. Varieties of technologies for detecting DNA methylation have been developed, but they are not sufficiently sensitive for use in diagnostic devices. The aim of this study was to determine the suitability of Raman spectroscopy for label-free detection of methylated DNA.

**Methods:** The methylated promoter regions of cancer-related genes cadherin 1 (*CDHI*) and retinoic acid receptor beta (*RARB*) served as target DNA sequences. Based on bisulfite conversion, oligonucleotides of methylated or nonmethylated probes and targets were synthesized for the DNA methylation assay. Principal component analysis with linear discriminant analysis (PCA-DA) was used to discriminate the hybridization between probes and targets (methylated probe and methylated target or nonmethylated probe and nonmethylated target) of *CDHI* and *RARB* from nonhybridization between the probe and targets (methylated probe and nonmethylated target or nonmethylated probe and methylated target).

**Results:** This study revealed that the *CDHI* and *RARB* oligo sets and their hybridization data could be classified using PCA-DA. The classification results for *CDHI* methylated probe + *CDHI* methylated target versus *CDHI* methylated probe + *CDHI* unmethylated target showed sensitivity, specificity, and error rates of 92%, 100%, and 8%, respectively. The classification results for the *RARB* methylated probe + *RARB* methylated target versus *RARB* methylated probe + *RARB* unmethylated target showed sensitivity, specificity, and error rates of 92%, 93%, and 11%, respectively.

**Conclusions:** Label-free detection of DNA methylation could be achieved using Raman spectroscopy with discriminant analysis.

**Key words:** DNA Methylation; Label-free Detection; Linear Discriminant Analysis; Principal Component Analysis; Raman Spectroscopy

## INTRODUCTION

DNA methylation is an essential component of epigenetics and plays a critical role in many biological events. DNA methylation in mammals has been observed in guanine-cytosine rich regions, also known as 5'-cytidine-phosphate-guanosine-3' (CpG) islands, which are frequently located in or near gene promoter regions. DNA methylation refers to the addition of methyl groups to cytosine nucleotides in the CpG islands of genes. Methylation of CpG islands can directly prevent transcription factor binding and lead to changes in the chromatin structure that restrict the access of transcription factors to the gene

promoter, causing silencing of gene expression.<sup>[1-3]</sup> Recent studies have shown that alterations in the DNA methylation of tumor-related genes might lead to cancer.<sup>[4,5]</sup> Thus, altered methylation of the promoters in several genes has been used as a biomarker for early cancer diagnosis and prognosis.<sup>[6-8]</sup>

**Address for correspondence:** Prof. Hun-Kuk Park, Department of Biomedical Engineering, College of Medicine, Kyung Hee University, Seoul 02447, Korea  
E-Mail: sigmoidus@khu.ac.kr

This is an open access article distributed under the terms of the Creative Commons Attribution-NonCommercial-ShareAlike 3.0 License, which allows others to remix, tweak, and build upon the work non-commercially, as long as the author is credited and the new creations are licensed under the identical terms.

**For reprints contact:** reprints@medknow.com

© 2017 Chinese Medical Journal | Produced by Wolters Kluwer - Medknow

**Received:** 03-02-2017 **Edited by:** Ning-Ning Wang  
**How to cite this article:** Kim J, Park HJ, Kim JH, Chang B, Park HK. Label-free Detection for a DNA Methylation Assay Using Raman Spectroscopy. Chin Med J 2017;130:1961-7.

### Access this article online

#### Quick Response Code:



**Website:**  
www.cmj.org

**DOI:**  
10.4103/0366-6999.211874

Various techniques for detecting DNA methylation patterns have been developed. Bisulfite conversion is commonly used to analyze gene-specific DNA methylation.<sup>[9]</sup> Treatment of DNA with bisulfite converts cytosine to uracil while leaving methylated cytosine intact; the methylated regions in DNA can then be detected as bisulfite-induced sequence differences.<sup>[9]</sup> Polymerase chain reaction (PCR)-based methods are routinely used to study DNA methylation on a gene-specific basis after bisulfite treatment, including bisulfite sequencing, methylation-specific PCR, real-time PCR-based MethyLight, and methylation-sensitive high-resolution melting PCR.<sup>[2]</sup> In addition, whole-epigenome profiling technologies can be used after bisulfite modification.<sup>[9]</sup> Identification of DNA methylation through bisulfite conversion does not require costly and complex instruments, enabling the analysis of specific single CpG sites. However, this approach may lead to false-positives and lacks sufficient sensitivity for direct screening of challenging samples with minimal DNA content.<sup>[10]</sup>

Raman spectroscopy has been extensively applied in the examination and characterization of molecular monolayers and various biological surfaces.<sup>[10-12]</sup> Previous studies<sup>[10,13-16]</sup> have detected DNA methylation by Raman spectroscopy. However, there are some limitations to the clinical application of Raman spectroscopy, such as the similarity of signals from single- and double-stranded DNA. To overcome those limitations, Wang *et al.*<sup>[15]</sup> proposed using embedded internal surface-enhanced Raman scattering (SERS) nanotags to quantify DNA. Several other approaches such as high-performance liquid chromatography and high-performance capillary electrophoresis have also been examined.<sup>[10]</sup> Raman spectroscopy is a label-free method with several advantages compared to fluorescence-based methods, because it can detect multiple sites of nucleoside methylation in DNA simultaneously.<sup>[10,15]</sup> In addition, no chemical additives are required, minimizing unexpected chemical changes in samples.<sup>[13,17]</sup> Raman bands represent molecular fingerprints with narrow bandwidths, enabling detection of multiple sites.<sup>[10,13]</sup>

This study evaluated label-free detection of DNA methylation based on bisulfite conversion to develop a sensitive and selective DNA methylation assay. We used methylated DNA probes to capture methylated targets, which were oligonucleotides from the promoter regions of

cancer-related genes (cadherin 1 [*CDH1*], and retinoic acid receptor beta [*RARB*]) as a detection model. Methylation and expression changes in *CDH1* and *RARB* in human cancers are well documented. *CDH1* is a cell adhesion molecule that plays an important role in cell growth and development.<sup>[18]</sup> The loss of function of this gene is thought to contribute to cancer progression. Downregulation of *CDH1* is correlated with decreased efficiency of cellular adhesion, which facilitates cellular motility to accelerate the invasion of surrounding tissues by cancer cells.<sup>[19]</sup> Increased methylation of *CDH1* has also been found in several cancers, suggesting that it is a causative factor for the loss of *CDH1* expression.<sup>[20]</sup> *RARB* is a member of the thyroid-steroid hormone receptor superfamily of nuclear transcriptional regulators. *RARB* binds retinoic acid, the biologically active form of vitamin A, which mediates cellular signaling in embryonic morphogenesis, cell growth, and differentiation. *RARB* expression is frequently lost in primary tumors and during metastasis compared to in adjacent noncancerous tissues.<sup>[21]</sup> Aberrant methylation of the *RARB* promoter has been observed in various malignant tumors including breast, colon, prostate, and lung cancers.<sup>[22,23]</sup> The purpose of this study was to discriminate DNA methylation from nonmethylation using Raman spectral data examined by multivariate principal component analysis with linear discriminant analysis (PCA-DA).

## METHODS

### Oligonucleotide design

Based on bisulfite modification methods, methylated probes containing methylated cytosine and nonmethylated probes containing thymine (T) rather than uracil were used as described previously.<sup>[24]</sup> Methylated and nonmethylated targets were complementary sequences of methylated and nonmethylated probes, respectively. Probe and target sequences in *CDH1* and *RARB* are shown in Table 1. All oligonucleotide sequences of probes and targets were customized by Macrogen Inc. (Seoul, Korea).

### Preparation of probe and target oligonucleotides

For Raman spectra analysis, oligonucleotides were dissolved in DNase- and RNase-free water at 100 pmol/L. Raman spectra of each methylated/nonmethylated target and probe were acquired after lyophilization of the

**Table 1: Sequences of probe and target oligonucleotides from genes *CDH1* and *RARB***

Gene	Name	Sequence
<i>CDH1</i>	Methylated probe (CMP)	5'-TAA TTT TAG GTT AGA GGG TTA TmCG mCG-3'
	Unmethylated (i.e., nonmethylated) probe (CUMP)	5'-TAA TTT TAG GTT AGA GGG TTA TTG TG-3'
	Methylated target (CMT)	5'-CG CGA TAA CCC TCT AAC CTA AAA TTA-3'
	Unmethylated target (CUMT)	5'-CA CAA TAA CCC TCT AAC CTA AAA TTA-3'
<i>RARB</i>	Methylated probe (RMP)	5'-GGT TAG TAG TTmCGGG TAG GGT TTA TmC-3'
	Unmethylated probe (RUMP)	5'- GGT TAG TAG TTTGGG TAG GGT TTA TT-3'
	Methylated target (RMT)	5'-GAT AAA CCC TAC CCG AAC TAC TAA CC-3'
	Unmethylated target (RUMT)	5'-AAT AAA CCC TAC CCA AAC TAC TAA CC-3'

*CDH1*: Cadherin 1; *RARB*: Retinoic acid receptor beta; mC: 5-methylcytosine.

dissolved oligonucleotides. To record the Raman spectra for binding or nonbinding of methylated/nonmethylated targets and probes, dissolved oligonucleotides of a methylated/nonmethylated target were added to those of methylated/nonmethylated probes at a 1:1 ratio and hybridized for 5 min at room temperature. The mixtures were stored at  $-70^{\circ}\text{C}$  and then lyophilized. Sequences of probe and target oligonucleotides from *CDH1* and their hybridization were abbreviated as follows: methylated probe (CMP), unmethylated probe (CUMP), methylated target (CMT), unmethylated target (CUMT), CMP + CMT, CMP + CUMT, CUMP + CMT, and CUMP + CUMT. Sequences of probe and target oligonucleotides from *RARB* and their hybridization were defined as follows: methylated probe (RMP), unmethylated probe (RUMP), methylated target (RMT), unmethylated target (RUMT), RMP + RMT, RMP + RUMT, RUMP + RMT, and RUMP + RUMT.

### Raman spectroscopy

Raman spectra of the bench top type were recorded on a spectroscope (Bruker Optics, Billerica, MA, USA) with a diode laser beam at an excitation wavelength of 785 nm. The benchtop Raman scattered light signal was collected with a  $\times 50$  object lens. The laser source with power 25 mW was focused on a SERS substrate with a spot diameter (or a sampling area) of  $2\ \mu\text{m}$ . All spectra were acquired at  $417\text{--}1782\ \text{cm}^{-1}$  at a spectral resolution  $0.5\ \text{cm}^{-1}$ . The acquisition time for *CDH1* and *RARB* was 60 s. The procedure was repeated five times to record the Raman spectra using a freeze-dried powder of each sample. Baseline correction was accomplished using OPUS 7.1 software (Bruker Optics Inc., Billerica, USA). The dataset was normalized to  $1002\ \text{cm}^{-1}$  without smoothing. Five results from repeated procedures from each normalized sample were averaged, and standard deviation was calculated for line plotting. The average was plotted as a solid line, while standard deviation was presented as a filled area.

### Statistical analysis

PCA was applied to the Raman spectra of the *CDH1* and *RARB* groups to distinguish the spectral features and classify

different samples. PCA was commonly used to qualitatively discriminate the patterns in data with many dimensions. Linear discriminant analysis (LDA) was then used for a two-group classification problem (quantitative discrimination of different pairwise reactions of hybridization). Sensitivity, specificity, and error could be calculated by LDA using the first three principal components. We calculated sensitivity as true-positives (TP)/(TP + false-positives [FN]), specificity as true-negatives (TN)/(TN + false-positives [FP]), and error as (FN + FP)/(FN + TN + FP + TP). PCA and LDA of the data were executed using the built-in R functions `prcomp()` and `lda()`. R version 3.2.5 originally developed at Bell Laboratories (Murray Hill, NJ, USA) was used. We performed LDA for two-group classification problems such as CMP + CMT versus CMP + CUMT, CUMP + CMT versus CUMP + CUMT, RMP + RMT versus RMP + RUMT, and RUMP + RMT versus RUMP + RUMT. To determine whether methylated probes of *CDH1* and *RARB* were specifically bound to only their methylated targets and not to their unmethylated targets, and that un-methylated probes were bound to only their un-methylated targets and not their methylated targets, the hybridization between methylated probe and methylated target was compared to that between the methylated probe and un-methylated target using PCA-DA. In addition, hybridization between un-methylated probes and un-methylated targets was compared to hybridization between un-methylated probes and methylated targets.

## RESULTS

Each methylated/nonmethylated probe and target from *CDH1* and *RARB* were analyzed by Raman spectroscopy to define the indicative spectral signatures of individual oligonucleotides (probes and targets) [Figures 1a and 2a]. After acquiring the Raman spectra of lyophilized samples, the spectra were normalized to the peak showing the highest intensity and offset for clarity. The spectral bands matched those reported previously for DNA identified by Raman peaks at  $497\ \text{cm}^{-1}$  (S-S stretch),  $599\ \text{cm}^{-1}$  ( $\text{N}_1\text{-H}$  [cytosine],  $\text{NH}_2$ ),  $620\ \text{cm}^{-1}$  (phenylalanine),  $679\ \text{cm}^{-1}$  (guanine),

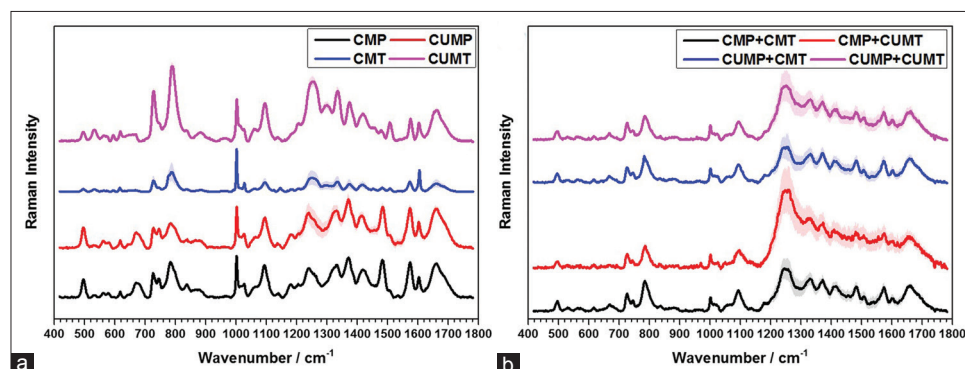


**Figure 1:** Raman spectra for target and probe oligonucleotides derived from *CDH1* (a), and for hybridization reactions of methylated/nonmethylated probes and targets (b). The thick lines show the average Raman spectra, whereas the shaded areas represent standard deviations. CMP: *CDH1* methylated probe; CMT: *CDH1* methylated target; CUMT: *CDH1* unmethylated target; CUMP: *CDH1* unmethylated probe; *CDH1*: Cadherin 1; *RARB*: Retinoic acid receptor beta.

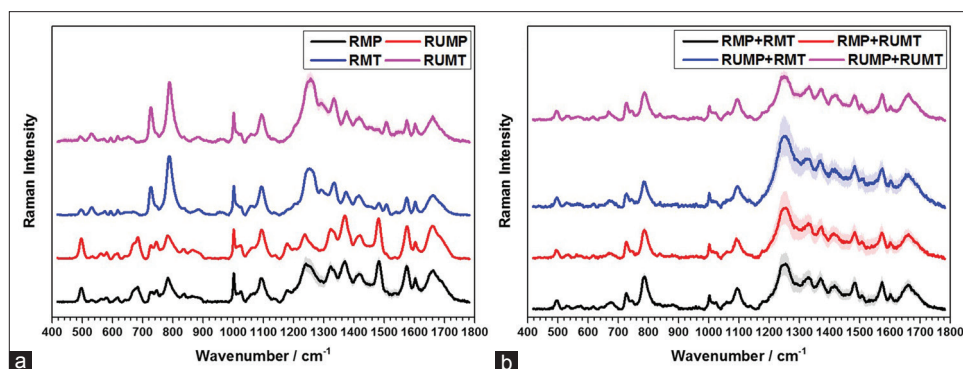


**Figure 2:** Raman spectra for target and probe oligonucleotides derived from *RARB* (a), and for hybridization reactions of methylated/nonmethylated probes and targets (b). The thick lines show the average Raman spectra, whereas the shaded areas represent standard deviations. RMP: *RARB* methylated probe; RMT: *RARB* methylated target; RUMT: *RARB* unmethylated target; RUMP: *RARB* unmethylated probe; *CDH1*: Cadherin 1; *RARB*: Retinoic acid receptor beta.

724  $\text{cm}^{-1}$  (DNA/RNA, adenine ring breathing), 747  $\text{cm}^{-1}$  (thymine), 780  $\text{cm}^{-1}$  (thymine), 1003  $\text{cm}^{-1}$  (symmetric ring breathing in phenylalanine), 1030  $\text{cm}^{-1}$  (phenylalanine), 1100  $\text{cm}^{-1}$  (C-C stretch [C, G, C(me)]), 1179  $\text{cm}^{-1}$  (thymine, cytosine), 1252  $\text{cm}^{-1}$  ( $\text{C}_6\text{-H}$ ,  $\text{N}_1\text{-H}$ ,  $\text{C}_5\text{-H}$  [cytosine]), 1336  $\text{cm}^{-1}$  (guanine), 1369  $\text{cm}^{-1}$  (guanine), 1420  $\text{cm}^{-1}$  (adenine, deoxyribose), 1478  $\text{cm}^{-1}$  (adenine), 1575  $\text{cm}^{-1}$  (pyrimidine rings [cytosine]), 1613  $\text{cm}^{-1}$  ( $\text{NH}_2$  bending,  $\text{C}_4\text{-NH}_2$  [cytosine]), and 1655  $\text{cm}^{-1}$  (C=O stretch  $\alpha$ -helix; amide I) [Table 2].<sup>[25-28]</sup> As shown in Figure 1a, the Raman spectra of CMP and CUMP showed similar patterns. The patterns of CMT and CUMT were also similar. In contrast, a difference in relative peak intensities was observed between CMP and CUMP at 724, 780, 837, and 1420  $\text{cm}^{-1}$ . The peak intensities of CMT were greater than those of CUMT across the Raman bands. These tendencies were also observed in the Raman spectra of RMP, RUMP, RMT, and RUMT [Figure 2a].

The Raman spectra of RMP and RUMP and those of RMT and RUMT were similar. In contrast, the peak intensities of the Raman spectra differed between RMP and RUMP at 497, 679, 1179, 1252, 1369, and 1478  $\text{cm}^{-1}$ . The peak intensity of RMT was greater than that of RUMT at 1478  $\text{cm}^{-1}$ . The differences in peak intensities may be because of differences in two oligonucleotides between methylated probes (cytosine) and nonmethylated probes (thymine) as well as between methyl targets (guanine) and nonmethylated targets (adenine). CMT and CUMP showed distinctive peaks at 747  $\text{cm}^{-1}$  and 1179  $\text{cm}^{-1}$ , respectively, while CMT and CUMT showed peaks at 1508  $\text{cm}^{-1}$ . Representative peaks of RMP, RUMP, RMT, and RUMT corresponded to the *CDH1* oligo sets.

To determine whether binding and nonbinding (or nonspecific binding) between probes and targets were distinguished by Raman spectroscopy, we recorded the Raman spectra after hybridization of methylated/nonmethylated probes and targets. The hybridization of methylated/nonmethylated probes and targets in *RARB* group was similar to those of *CDH1* oligo sets [Figure 1b]. After hybridization of RMP with either RMT or RUMT [Figure 2b], the relative peak intensities of Raman spectra of RMP + RMT and RMP + RUMT differed at 679, 780, 1100, and 1575  $\text{cm}^{-1}$ .

**Table 2: Raman peak positions and assignment of major vibrational bands observed in *CDH1* or *RARB* oligo sets and their hybridization detected by Raman spectroscopy**

Peak position ( $\text{cm}^{-1}$ )	Assignment
497	S-S stretch
599	$\text{N}_1\text{-H}$ (cytosine), $\text{NH}_2$
620	Phenylalanine
679	Guanine
724	DNA/RNA (adenine ring breathing)
747	Thymine
780	Thymine
1003	Symmetric ring breathing in phenylalanine
1030	Phenylalanine
1100	C-C stretch (C, G, C[me])
1179	Thymine, cytosine
1252	$\text{C}_6\text{-H}$ , $\text{N}_1\text{-H}$ , $\text{C}_5\text{-H}$ (cytosine)
1336	Guanine
1369	Guanine
1420	Adenine, deoxyribose
1478	Adenine
1575	Pyrimidine rings (cytosine)
1613	$\text{NH}_2$ bending, $\text{C}_4\text{-NH}_2$ (cytosine)
1665	C=O stretch $\alpha$ -helix; Amide I

*CDH1*: Cadherin 1; *RARB*: Retinoic acid receptor beta; mC: 5-methylcytosine.

Figure 2b shows that the Raman spectra of RUMP hybridized with either RMT or RUMT appeared similar, but the Raman spectra of RUMP + RMT showed higher intensity than that of RUMP + RUMT between 1100 and 1782  $\text{cm}^{-1}$ .

We performed PCA on *CDH1* oligo sets and their hybridization reactions [Figure 3a]. Six groups (CMP, CUMP, CMT, CUMT, CMP + CMT, and CMP + CUMT) were distinctly classified, while the boundary between the CUMP + CMT group and CUMP + CUMT group was ambiguous. We evaluated two PCA tests to determine whether we could define a boundary between CMP + CMT and CMP + CUMT or between CUMP + CMT and CUMP + CUMT. Figure 3b and 3c show that each



hybridization reaction was clearly classified, depending on binding and nonbinding (or nonspecific binding). We also conducted PCA for *RARB* oligo sets and their hybridization reactions. Figure 4a shows that four hybridized samples (RMP + RMT, RMP + RUMT, RUMP + RMT, and RUMP + RUMT) had ambiguous boundaries. To classify these samples, we conducted PCA for RMT or RUMT hybridized with RMP and were able to distinguish the boundaries, as shown in Figure 4b. Similarly, the PCA results for RMT or RUMT hybridized to RUMP were sufficiently different [Figure 4c].

Table 3 shows the classification results for two-group classification problems such as CMP + CMT versus CMP + CUMT, CUMP + CMT versus CUMP + CUMT, RMP + RMT versus RMP + RUMT, and RUMP + RMT versus RUMP + RUMT using PCA-DA. After PCA for four two-group classifications, sensitivity, specificity, and error were calculated by LDA using the first three principal components [Figures 3b, 3c and 4b, 4c]. The classification data yielded the best results for sensitivity, specificity, and error with values of 94%, 92%, and 13%, respectively.

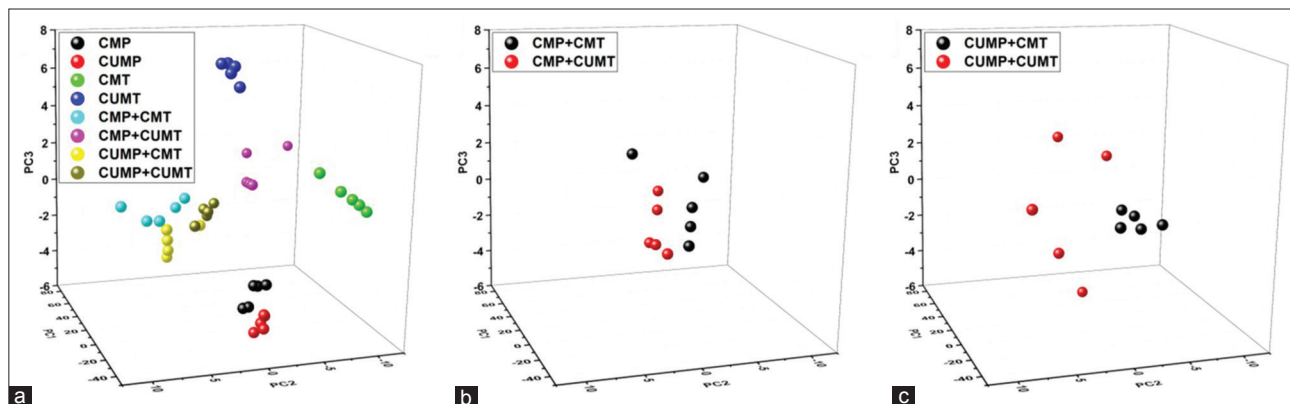


**Figure 3:** Principal component analysis for target and probe oligonucleotides of group *CDH1* and hybridization reactions of methylated/nonmethylated probes and targets (a), CMT and CUMT hybridized with CMP (b), and CMT and CUMT hybridized with CUMP (c). CMP: *CDH1* methylated probe; CMT: *CDH1* methylated target; CUMT: *CDH1* unmethylated target; CUMP: *CDH1* unmethylated probe; *CDH1*: Cadherin 1; *RARB*: Retinoic acid receptor beta.

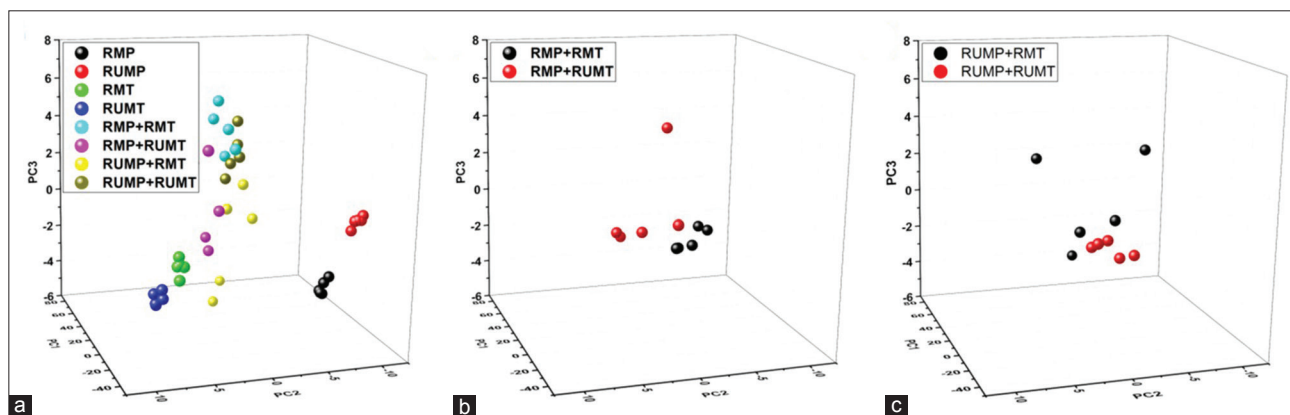


**Figure 4:** Principal component analysis for target and probe oligonucleotides of group *RARB* and hybridization reactions of these methylated/nonmethylated probes and targets (a), RMT and RUMT hybridized with RMP (b), and RMT and RUMT hybridized with RUMP (c). RMP: *RARB* methylated probe; RMT: *RARB* methylated target; RUMT: *RARB* unmethylated target; RUMP: *RARB* unmethylated probe; *CDH1*: Cadherin 1; *RARB*: Retinoic acid receptor beta.

**Table 3: Classification of results of Raman prediction using PCA-DA**

Parameters	Sensitivity (%)	Specificity (%)	Error (%)
CMP + CMT versus CMP + CUMT	92	100	8
CUMP + CMT versus CUMP + CUMT	91	91	15
RMP + RMT versus RMP + RUMT	92	93	11
RUMP + RMT versus RUMP + RUMT	100	82	19

CMP: *CDH1* methylated probe; CMT: *CDH1* methylated target; CUMT: *CDH1* unmethylated target; CUMP: *CDH1* unmethylated probe; RMP: *RARB* methylated probe; RMT: *RARB* methylated target; RUMT: *RARB* unmethylated target; RUMP: *RARB* unmethylated probe; *CDH1*: Cadherin 1; *RARB*: Retinoic acid receptor beta; PCA-DA: Principal component analysis with linear discriminant analysis.

## DISCUSSION

CpG methylation in the promoter region of a gene has been reported to contribute to tumorigenesis, corresponding to the gain of function of oncogenes and loss of function of tumor suppressor genes.<sup>[29]</sup> Accordingly, DNA methylation has been recognized as a biomarker for identifying cancer etiology, particularly during early stages, and monitoring the progression of malignant tumors.<sup>[30]</sup> In the present study, we detected DNA methylation patterns of the cancer-related genes *CDHI* and *RARB* using Raman spectroscopy and PCA-DA, which cannot be qualitatively differentiated only by Raman spectra or PCA. The PCA-DA developed for DNA methylation analysis in this study showed that methylated targets were detected with high sensitivity and specificity. Previous studies also demonstrated the usefulness of PCA-DA to qualitatively classify Raman data to compare two groups. Choi *et al.*<sup>[31]</sup> utilized PCA-DA to differentiate plasma-treated cells from control cells. Their classification results were accurate, sensitive, and specific (91%, 87%, and 99%, respectively). Liu *et al.*<sup>[32]</sup> measured Raman spectra of human colorectal tissue samples and employed PCA-LDA to discriminate cancerous from normal tissues, showing a diagnostic accuracy of 79.2%. Accuracy and sensitivity may further be improved by introducing non-LDA such as quadratic or orthogonal quadratic discriminant functions.<sup>[32,33]</sup> In the future studies, we plan to quantify multiple methylation proportions for early cancer detection and treatment. Furthermore, experimental and clinical DNA samples from a variety of cancer cell lines and tissues from cancer patients will be included to verify the accuracy and utility of label-free Raman detection in a DNA methylation assay.<sup>[34]</sup>

In conclusion, we collected Raman spectra for *CDHI* and *RARB* oligo sets and their hybridizations to detect DNA methylation. We also used PCA to classify CMT and CUMT hybridized with CMP, and RMT and RUMT hybridized with RMP. The PCA results showed that DNA methylation and nonmethylation of cancer-related genes can be discriminated by Raman spectroscopy by analyzing the binding or nonbinding of specific probes. Therefore, label-free detection of DNA methylation in marker genes was achieved by Raman spectroscopy. This technique is useful for developing point-of-care medical devices for early cancer diagnosis.

## Financial support and sponsorship

Nil.

## Conflicts of interest

There are no conflicts of interest.

## REFERENCES

1. Baylin SB, Jones PA. A decade of exploring the cancer epigenome – Biological and translational implications. *Nat Rev Cancer* 2011;11:726-34. doi: 10.1038/nrc3130.
2. Fraga MF, Esteller M. DNA methylation: A profile of methods and applications. *Biotechniques* 2002;33:632-49.
3. Feinberg AP, Vogelstein B. Hypomethylation distinguishes genes

- of some human cancers from their normal counterparts. *Nature* 1983;301:89-92. doi: 10.1038/301089a0.
4. Esteller M. CpG island hypermethylation and tumor suppressor genes: A booming present, a brighter future. *Oncogene* 2002;21:5427-40. doi: 10.1038/sj.onc.1205600.
5. Robertson KD, Wolffe AP. DNA methylation in health and disease. *Nat Rev Genet* 2000;1:11-9. doi: 10.1038/35049533.
6. Laird PW. The power and the promise of DNA methylation markers. *Nat Rev Cancer* 2003;3:253-66. doi: 10.1038/nrc1045.
7. Yu J, Cheng YY, Tao Q, Cheung KF, Lam CN, Geng H, *et al.* Methylation of protocadherin 10, a novel tumor suppressor, is associated with poor prognosis in patients with gastric cancer. *Gastroenterology* 2009;136:640-51. doi: 10.1053/j.gastro.2008.10.050.
8. Müller HM, Widschwendter A, Fiegl H, Ivarsson L, Goebel G, Perkmann E, *et al.* DNA methylation in serum of breast cancer patients: An independent prognostic marker. *Cancer Res* 2003;63:7641-5.
9. Wani K, Aldape KD. PCR techniques in characterizing DNA methylation. *Methods Mol Biol* 2016;1392:177-86. doi: 10.1007/978-1-4939-3360-0\_16.
10. Hu J, Zhang CY. Single base extension reaction-based surface enhanced Raman spectroscopy for DNA methylation assay. *Biosens Bioelectron* 2012;31:451-7. doi: 10.1016/j.bios.2011.11.014.
11. Liu R, Zhu S, Si M, Liu Z, Zhang D. Surface-enhanced Raman scattering-based approach for DNA detection at low concentrations via polyvinyl alcohol-protected silver grasslike patterns. *J Raman Spectrosc* 2012;43:370-9.
12. Talari A, Evans C, Holen I, Coleman R, Rehman IU. Raman spectroscopic analysis differentiates between breast cancer cell lines. *J Raman Spectrosc* 2015;46:421-7. doi: 10.1002/jrs.4676.
13. Wang Y, Wee EJ, Trau M. Accurate and sensitive total genomic DNA methylation analysis from sub-nanogram input with embedded SERS nanotags. *Chem Commun (Camb)* 2016;52:3560-3. doi: 10.1039/c6cc00547k.
14. Barhoumi A, Halas NJ. Detecting chemically modified DNA bases using surface enhanced Raman spectroscopy. *J Phys Chem Lett* 2011;2:3118-23. doi: 10.1021/jz201423b.
15. Wang Y, Wee EJ, Trau M. Highly sensitive DNA methylation analysis at CpG resolution by surface-enhanced Raman scattering via ligase chain reaction. *Chem Commun (Camb)* 2015;51:10953-6. doi: 10.1039/c5cc03921e.
16. Guerrini L, Krpetic Ž, van Lierop D, Alvarez-Puebla RA, Graham D. Direct surface-enhanced Raman scattering analysis of DNA duplexes. *Angew Chem Int Ed Engl* 2015;54:1144-8. doi: 10.1002/anie.201408558.
17. Zhou Z, Han X, Huang GG, Ozaki Y. Label-free detection of binary mixtures of proteins using surface-enhanced Raman scattering. *J Raman Spectrosc* 2012;43:706-11. doi: 10.1002/jrs.3085.
18. Shiozaki H, Oka H, Inoue M, Tamura S, Monden M. E-cadherin mediated adhesion system in cancer cells. *Cancer* 1996;77 8 Suppl: 1605-13. doi: 10.1002/(SICI)1097-0142(19960415)77:8<1605::AID-CNCR28>3.0.CO;2-2.
19. Tzanou E, Peschos D, Batistatou A, Charalabopoulos A, Charalabopoulos K. The E-cadherin adhesion molecule and colorectal cancer. A global literature approach. *Anticancer Res* 2008;28:3815-26.
20. Bornman DM, Mathew S, Alsrube J, Herman JG, Gabrielson E. Methylation of the E-cadherin gene in bladder neoplasia and in normal urothelial epithelium from elderly individuals. *Am J Pathol* 2001;159:831-5. doi: 10.1016/S0002-9440(10)61758-0.
21. Mehrotra J, Vali M, McVeigh M, Kominsky SL, Fackler MJ, Lahti-Domenici J, *et al.* Very high frequency of hypermethylated genes in breast cancer metastasis to the bone, brain, and lung. *Clin Cancer Res* 2004;10:3104-9. doi: 10.1158/1078-0432.CCR-03-0118.
22. Moison C, Assemat F, Daunay A, Tost J, Guieysse-Peugeot AL, Arimondo PB. Synergistic chromatin repression of the tumor suppressor gene *RARB* in human prostate cancers. *Epigenetics* 2014;9:477-82. doi: 10.4161/epi.27869.
23. Virmani AK, Rathi A, Zöchbauer-Müller S, Sacchi N, Fukuyama Y, Bryant D, *et al.* Promoter methylation and silencing of the retinoic

- acid receptor-beta gene in lung carcinomas. *J Natl Cancer Inst* 2000;92:1303-7.
24. Shin Y, Perera AP, Kee JS, Song J, Fang Q, Lo GQ, *et al.* Label-free methylation specific sensor based on silicon microring resonators for detection and quantification of DNA methylation biomarkers in bladder cancer. *Sens Actuators B* 2013;177:404-11. doi: 10.1016/j.snb.2012.11.058.
  25. Kelly JG, Najand GM, Martin FL. Characterisation of DNA methylation status using spectroscopy (mid-IR versus Raman) with multivariate analysis. *J Biophotonics* 2011;4:345-54. doi: 10.1002/jbio.201000085.
  26. Pandya AK, Serhatkulu GK, Cao A, Kast RE, Dai H, Rabah R, *et al.* Evaluation of pancreatic cancer with Raman spectroscopy in a mouse model. *Pancreas* 2008;36:e1-8. doi: 10.1097/MPA.0b013e31815a3f1c.
  27. Schulze HG, Konorov SO, Piret JM, Blades MW, Turner RF. Label-free imaging of mammalian cell nucleoli by Raman microspectroscopy. *Analyst* 2013;138:3416-23. doi: 10.1039/c3an00118k.
  28. An JH, Choi DK, Lee KJ, Choi JW. Surface-enhanced Raman spectroscopy detection of dopamine by DNA targeting amplification assay in Parkinson's model. *Biosens Bioelectron* 2015;67:739-46. doi: 10.1016/j.bios.2014.10.049.
  29. Ng JM, Yu J. Promoter hypermethylation of tumour suppressor genes as potential biomarkers in colorectal cancer. *Int J Mol Sci* 2015;16:2472-96. doi: 10.3390/ijms16022472.
  30. Fernandez AF, Assenov Y, Martin-Subero JI, Balint B, Siebert R, Taniguchi H, *et al.* A DNA methylation fingerprint of 1628 human samples. *Genome Res* 2012;22:407-19. doi: 10.1101/gr.119867.110.
  31. Choi JS, Kim J, Hong YJ, Bae WY, Choi EH, Jeong JW, *et al.* Evaluation of non-thermal plasma-induced anticancer effects on human colon cancer cells. *Biomed Opt Express* 2017;8:2649-59. doi: 10.1364/BOE.8.002649.
  32. Liu W, Sun Z, Chen J, Jing C. Raman spectroscopy in colorectal cancer diagnostics: Comparison of PCA-LDA and PLS-DA models. *J Spectrosc* 2016. doi: 10.1155/2016/1603609.
  33. Stables R, Clemens G, Butler HJ, Ashton KM, Brodbelt A, Dawson TP, *et al.* Feature driven classification of Raman spectra for real-time spectral brain tumour diagnosis using sound. *Analyst* 2016;142:98-109. doi: 10.1039/c6an01583b.
  34. Feng S, Wang W, Tai IT, Chen G, Chen R, Zeng H. Label-free surface-enhanced Raman spectroscopy for detection of colorectal cancer and precursor lesions using blood plasma. *Biomed Opt Express* 2015;6:3494-502. doi: 10.1364/BOE.6.003494.